Vibrational Förster transfer to hydrated protons

Timmer, R.L.A.; Tielrooij, K.J.; Bakker, H.J.

DOI
10.1063/1.3432616
Publication date
2010
Document Version
Final published version
Published in
Journal of Chemical Physics

Vibrational Förster transfer to hydrated protons

R. L. A. Timmer,[a] K. J. Tielrooij, and H. J. Bakker
FOM-institute for Atomic and Molecular Physics, Kruislaan 407, 1098 SJ Amsterdam, The Netherlands

(Received 29 October 2009; accepted 3 May 2010; published online 21 May 2010)

We have studied the influence of excess protons on the vibrational energy relaxation of the O–H and O–D stretching modes in water using femtosecond pump-probe spectroscopy. Without excess protons, we observe exponential decays with time constants of 1.7 and 4.3 ps for the bulk and anion bound O–D stretch vibrations. The addition of protons introduces a new energy relaxation pathway, which leads to an increasingly nonexponential decay of the O–D stretch vibration. This new pathway is attributed to a distance-dependent long range dipole-dipole (Förster) interaction between the O–D stretching vibration and modes associated with dissolved protons. The high efficiency of hydrated protons as receptors of vibrational energy follows from the very large absorption cross section and broad bandwidth of protons in water. For a proton concentration of 1*M* we find that Förster energy transfer occurs over an average distance of 4.5 Å, which corresponds to a separation of about two water molecules. © *2010 American Institute of Physics*. [doi:10.1063/1.3432616]

I. INTRODUCTION

Water plays an essential role as mediator and active participant in a wide variety of chemical interactions. In biology it is sometimes referred to as the "lubricant of life"[1] due to its ubiquitous presence and its ability to facilitate crucial interactions ranging from the passing of ions to the folding of proteins.[2] Many important properties of water can be attributed to its polar nature which allows it to form hydrogen bonds with other molecules and ions. Despite the high density and strength of these bonds, water shows surprisingly fast rearrangements in its hydrogen bond network which facilitates the redistribution of excess energies.[3–6] Energy relaxation in water consists of both intra- and intermolecular energy transfer[7,8] pathways. In general, the dissipation rate of (vibrational) energy depends on the number density and coupling strength of accepting modes that are present in proximity to the excited oscillator. The main transfer mechanism within molecules consists of anharmonic couplings between molecular modes. In liquids, such as water, the frequencies of these modes are continuously modulated through variations in the hydrogen bond distance, strength, and angle.[9,10] Resonant energy transfer between molecules is also possible through a direct dipole-dipole coupling mechanism, called Förster energy transfer.[11] In this mechanism the donor and acceptor molecules are within an interaction length much smaller than the wavelength of the transition, leading to the exchange of a virtual photon (nonradiative).

A technique well suited for the study of the dynamics of aqueous systems on the subpicosecond time scale is nonlinear vibrational spectroscopy.[12–17] Previous studies on pure liquid water have shown that Förster type interactions between water molecules lead to vibrational energy transfer on a time scale <100 fs.[3,5] Similar interactions have been observed for the amide vibrations of peptides[18] and for vibrations of adsorbed molecules.[19] Characteristic for these observations is, that the energy remains in the same type of molecular vibration, e.g., the O–H stretch vibrations of water molecules or the amide modes of peptides. Here we demonstrate the presence of Förster energy transfer between the O–D stretch mode and hydrated protons. The addition of protons to water gives rise to new vibrational modes associated with various complexes of water involving excess protons.[20] The most well known are the so-called Eigen[21] ($H_9O_4^+$) and Zundel[22] ($H_5O_2^+$) modes that involve protons solvated by four and two water molecules, respectively. A previous study[23] that directly probed the vibrational relaxation of the Eigen and Zundel proton hydration complexes revealed that the relaxation is much faster than that of normal water (100 fs compared to 700 fs).

The goal of this study is to find the influence of excess protons on the molecular energy dynamics of water molecules. We use femtosecond midinfrared pump-probe laser pulses to measure the rate at which hydrated protons accept the energy of a nearby vibrational excitation. Although we are primarily interested here in bulk water behavior, we will also study the fraction of water molecules bound to the anion that inevitably accompanies the excess proton.

II. EXPERIMENT

A. Pump-probe spectroscopy

The vibrational energy relaxation and orientational dynamics of the O–H and O–D stretch vibrations in water were studied with pump-probe spectroscopy. The pump and probe pulses were generated via a sequence of nonlinear frequency-conversion processes described elsewhere.[24] Their central frequencies were in the regions around 2500 and 3400 cm^{-1}, coinciding with the O–D and O–H stretch modes, respectively. The pump and probe pulses with a full width at half maximum of about 200 cm^{-1} had pulse energies of 5 μJ and 20 nJ, respectively. We measured the pump-induced frequency-resolved transient absorption spectra ($\Delta\alpha$) of various samples as a function of time delay between pump and

[a]Electronic mail: r.timmer@amolf.nl.

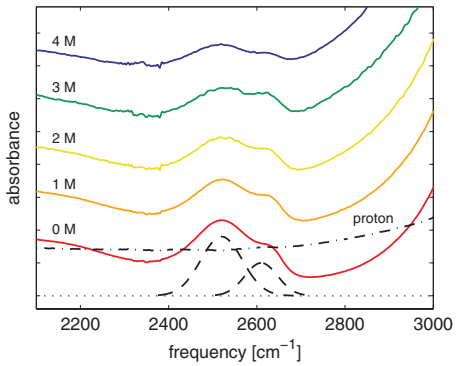

FIG. 1. Linear absorption spectra of aqueous mixtures containing varying relative amounts of $NaClO_4$ and $HClO_4$. From bottom to top, the concentrations of $HClO_4$:$NaClO_4$ are 0:4, 1:3, 2:2, 3:1, and 4:0. The different offsets are caused by the broadband absorption of the increasing proton concentrations. The two bands around 2520 and 2610 cm^{-1} (dashed lines) are assigned to the O–D stretch vibrations of bulk and anion bound water, respectively. The dash-dotted line shows the absorption cross section of the dissolved proton, obtained by taking the difference spectra between subsequent acid concentrations.

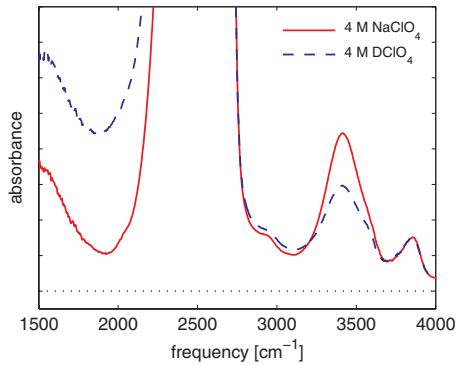

FIG. 2. Linear spectra of aqueous mixtures containing 4*M* $NaClO_4$ (solid line) and 4*M* $DClO_4$ (dashed line). This figure shows the lack of vibrational overlap between the O–H stretch vibration around 3400 cm^{-1} and the dissolved deuteron at frequencies below 2500 cm^{-1}.

probe. The relative polarizations of pump and probe were set to magic angle (54.7°) to determine the dynamics of the vibrational relaxation processes, independent of the (changing) direction of the transition dipole moments. The instrument response time was about 150 fs.

The pump promotes population from the ground state $\nu=0$ to the first excited state, $\nu=1$. This excitation is observed as a bleach and stimulated emission at frequencies matching $\nu=0\rightarrow1$, and an induced absorption at frequencies matching $\nu=1\rightarrow2$. The latter transition will lie at a lower frequency for anharmonic oscillators such as the O–H stretching mode of water. Together these transitions provide a spectral signature that allows for the tracking of the population of the $\nu=1$ state. Decay of the O–H or O–D stretch modes leads to a thermalized end state that. This thermalization leads to the occupation of low frequency modes that manifests itself as a decreased and blueshifted absorption spectrum of the O–H or O–D stretch mode[25] (e.g., see Fig. 4, "heat").

B. Samples under study

The samples consisted of various mixtures of sodium perchlorate ($NaClO_4$) and perchloric acid ($HClO_4$) dissolved in isotopically diluted (8%) aqueous solutions of either HDO in H_2O or HDO in D_2O. These mixtures had molar ratios 4:0, 3:1, 2:2, 1:3, and 0:4 (see Fig. 1), meaning that the amount of perchlorate was kept constant (4*M*), while the acid concentration varied between 0 and 4*M*. This was done to exclude the influence of the anion on any comparative observations. The sample cell had an optical path length of 25 μm. Figure 1 shows two distinct absorptions bands. The absorption around 2520 cm^{-1} is associated with the O–D stretch of HDO, hydrogen bonded to the oxygen of another water molecule. The other band, in the region around 2610 cm^{-1} is the result of O–D stretch oscillators that are hydrogen bonded to perchlorate ions.[26] This band is blueshifted which indicates that water forms weaker hydrogen bond to perchlorate anions than to water. This spectral separation is important because it allows us to deconvolve the behavior of bulk and anion-bound water. The sodium cation has been shown[27,28] to have negligible effects on both the relaxation and reorientation time of water molecules.

Perchloric acid belongs to the class of so-called super acids, having a $pK_a=-7$. This means that the amount of dissolved protons (or deuterons) can be assumed to increase linearly with the amount of dissolved acid. Figure 1 shows that the increasing proton concentration gives rise to a large broadband background signal which was isolated by taking the difference spectrum between various acid concentrations (dash-dotted line). This background can be assigned to a wide variety of hydrated proton vibrations, among which the most well known are the modes of the so-called Eigen[21] (H_3O^+) and Zundel[22] ($H_5O_2^+$) structures.

The absorbance of the O–D vibration near 2550 cm^{-1} is observed to decrease with increasing acid concentration. This decrease is not a result of a change in isotope ratio D/H as this ratio was kept constant at 4% taking into account the added protons from $HClO_4$. Instead, the decrease is due to the frequency shift of O–D oscillators that are participating in the solvation of the excess proton, such as those appearing in DH_2O^+ and $DH_4O_2^+$ complexes. The frequencies of these oscillators will be strongly redshifted due to the added proton. As a result, these O–D groups vanish from the absorption bands near 2550 cm^{-1}.

In Fig. 2, linear spectra of the reciprocal system, i.e., $NaClO_4$ and $DClO_4$ dissolved in an isotopically diluted solution of 4% HDO in D_2O are presented. Shown are two spectra, with molar ratios of $NaClO_4$ and $DClO_4$ of 4:0 and 0:4. It is clearly seen that the O–H stretch absorption bands of HDO at ~3500 cm^{-1} do not spectrally overlap with the broadband continuum of the hydrated deuteron vibrations (<2500 cm^{-1}). In addition, it is observed that the absorbance of the O–H stretch vibrations near 3500 cm^{-1} decreases with increasing acid concentration, because a significant fraction of the O–H groups undergoes a large frequency redshift when participating in solvation structures of the deuteron (HD_2O^+ and $HD_4O_2^+$). In both Figs. 1 and 2, we observe a 30% drop in absorbance upon addition of 4*M* of acid. This indicates that 4*M* protons/deuterons affect about 30% of the O–D and O–H groups in the solution, which have a total

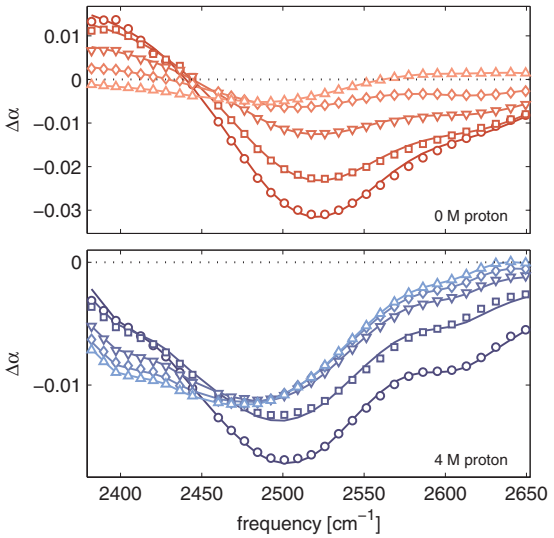

FIG. 3. Transient absorption spectra showing the O–D stretching modes of $4M$ $NaClO_4$ (top) and $4M$ $HClO_4$ (bottom). Data is shown for pump-probe delays of 0.4 (circles), 1 (squares), 2 (downward triangles), 4 (diamonds), and 100 ps (upward triangles). The lines show the Gaussian fits used to calculate the population per mode.

concentration of about $110M$. Thus a single deuteron/proton affects the frequency of about $8(=0.30\times 110/4)$ surrounding O–D and O–D groups. This number is close to what one would expect for a $H_nD_{9-n}O_4^+$ (Ref. 21) solvation structure, suggesting that this structure dominates.

III. RESULTS AND DISCUSSION

A. Transient spectra

Figure 3 shows two isotropic pump-probe measurements on the O–D stretch vibrations in aqueous solutions of $4M$ sodium perchlorate (top) and $4M$ perchloric acid (bottom). Both panels show a structure of two negative bands, corresponding to the pump induced bleach of the ground state and stimulated emission from the first excited state. Not visible in this figure is the lower frequency induced absorption resulting from transitions between the first and second excited states. This induced absorption can be observed when going to lower frequencies.

The main difference between the two data sets is the considerably faster decay of both bands in the protonated sample. Comparing the linear spectra (Fig. 1) of these two samples we note the broad background absorption due to these proton associated modes. An obvious speculation, at this point, is that these protons are somehow facilitating the vibrational relaxation of the O–D stretch modes. The exact mechanism for this relaxation pathway is what we will investigate.

A previous study on HDO in H_2O has shown[29] that the transient line shape of the O–D stretch vibration has a large width already at early delays. This finding implies that the O–D absorption band possesses significant homogeneous broadening and/or that most of the spectral diffusion processes takes place on a very short time scale (<50 fs). As a result, the effects of spectral diffusion will be small at delays <1 ps and negligible for delays >1 ps. Moreover, the spectrum of the excitation pulse is quite broad (150 cm^{-1}) which will further reduce the effects of spectral diffusion. We can therefore describe our data using a set of spectra with time-independent shapes.

We start our analysis by modeling the simplest case of the sample without added protons (top Fig. 3). From a singular value decomposition[30] on the data matrix $\Delta\alpha_{iso}(t,\nu)$, we find that these data are well described ($>96\%$) using a three component model where each component is the product of a time evolving population $N(t)$ and a corresponding spectral signature $\sigma(\nu)$

$$\Delta\alpha_{iso}(t,\nu) = N_b(t)\cdot\sigma_b(\nu) + N_a(t)\cdot\sigma_a(\nu) + N_{0^*}(t)\cdot\sigma_{0^*}(\nu). \tag{1}$$

The first component consists of O–D stretch oscillators in the first excited state that donate hydrogen bonds to other water molecules. This component gives rise to a decreased absorption around 2520 cm^{-1} and will be referred to as "bulk" water, b. The second component consists of O–D stretch oscillators in the first excited state that are hydrogen bonded to the perchlorate anion. This blueshifted absorption band, around 2610 cm^{-1}, will be referred to as the anion-bound water a and decays with a much slower time scale. Finally there are molecules residing in a heated thermalized ground state, referred to as 0^*. The thermalization of the energy of the excitation leads to a blueshifted ground-state spectrum as a result of anharmonic coupling between low frequency modes to the O–D stretch vibration. Its spectral signature can be directly observed at later time delays (100 ps) and its population increases as the other two modes decay.

We thus construct a kinetic model that assumes two separate components, bulk and anion-bound, each decaying with a different rate (k_b and k_a) toward a thermalized end-state. Rate equations that describe the populations in bulk ($N_b(t)$), anion-bound ($N_a(t)$) and thermalized end-state ($N_{0^*}(t)$) can be written as

$$\frac{d}{dt}\begin{pmatrix} N_b(t) \\ N_a(t) \\ N_{0^*}(t) \end{pmatrix} = \begin{bmatrix} -k_b & 0 & 0 \\ 0 & -k_a & 0 \\ k_b & k_a & 0 \end{bmatrix}\begin{pmatrix} N_b(t) \\ N_a(t) \\ N_{0^*}(t) \end{pmatrix}. \tag{2}$$

The solutions $N_b(t)$, $N_a(t)$, and $N_{0^*}(t)$ are a function of rate constants k_b and k_a and initial conditions $N_b(0)$, $N_a(0)$, and $N_{0^*}(0)$. These two rate constants are fitted to the data in combination with least-squares calculated spectra $\sigma_b(\nu)$, $\sigma_a(\nu)$ and $\sigma_{0^*}(\nu)$. This spectral decomposition calculation is explained in Appendix.

Figure 4 shows the shape of the spectra (markers) for the initial conditions $N_b(0)=0.5$, $N_a(0)=0.5$, and $N_{0^*}(0)=0$. These spectral signatures look as expected, when compared to the linear spectrum of Fig. 1. We find that the bulk decay rate k_b corresponds to a time constant around 1.7 ps, the same as was found in a previous study[6] for neat HDO in H_2O. The anion-bound decay rate k_a corresponds to a significantly slower time constant of around 4.3 ps.

In the previous description of the relaxation dynamics we have neglected the exchange between the bulk and anion-bound species. This exchange was recently measured[31] to be on a time scale of ~ 9 ps. This means that it is slow in

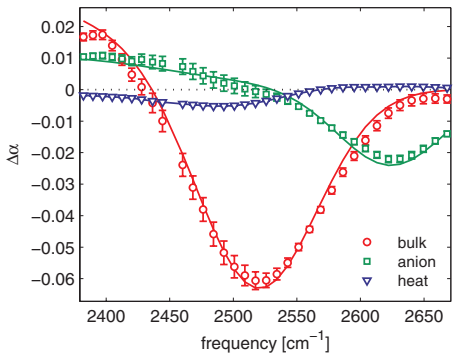

FIG. 4. Decomposed spectra $\sigma_b(\nu)$, $\sigma_a(\nu)$, and $\sigma_{0^*}(\nu)$. Markers show the least-squares decomposed spectra using a kinetic fitting model on the $4M$ $NaClO_4$, HDO in H_2O sample. The bulk and anion-bound O–D stretching modes are shown with circles and squares, respectively, and the thermalized end spectrum is shown with triangles. The lines show the Gaussian fits resulting from the global analysis used to calculate the time dependent population per mode.

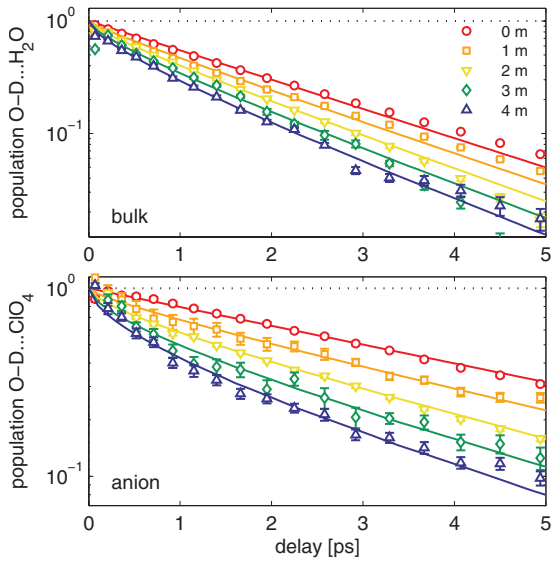

FIG. 5. Population dynamics for bulk (top) and anion-bound (bottom) water (O–D vibration of HDO in H_2O). Markers show the least-squares decomposed populations for increasing proton concentrations from 0 up to $4M$. The lines are a global fit, described in the text, which finds a bulk rate k_b=0.6 ps^{-1} and anion-bound rate k_a=0.23 ps^{-1}. The Förster transfer rate k_F=1450 ps^{-1} $Å^6$ and the minimum transfer radius a_0=1.5 Å.

comparison to the vibrational relaxation of the two species, and can be neglected in the description of the dynamics. It should also be pointed out that in case the exchange would have been fast, this would have led to a rapid equilibration of the two species and a decay with the same averaged relaxation rate at longer delay times. This is not what we observe, since at all delay times the decay rates are clearly different, thus confirming that the exchange must be slow.

We now wish to continue the analysis of the solutions containing $HClO_4$. However, because we do not know, *a priori*, how the added protons affect the vibrational equilibration pathways, we will instead make use of the acquired knowledge of the constituent spectra $\sigma_b(\nu)$ and $\sigma_a(\nu)$. These spectra are assumed to be similar across all acid concentrations. So instead of modeling the population dynamics and calculating the least-squares fitting spectra, we will fit the spectra and calculate the least-squares fitting population dynamics (temporal decomposition, Appendix). Thereby we can decompose the population dynamics without prior knowledge of the relaxation model.

We use the decomposed spectra from Fig. 4 as a starting point to construct spectra for the bulk and anion-bound O–D vibration bands. For simplicity we will use two Gaussian bands for each spectrum. One negative band ($\Delta\alpha<0$), corresponding to bleach and stimulated emission at $\nu=0\rightarrow1$, and one positive band ($\Delta\alpha>0$) corresponding to induced absorption at $\nu=1\rightarrow2$. For each data set, we furthermore extract the thermalization spectrum that we get at late time delays. The three spectra (bulk, anion-bound, thermalization) are then used to find the least-squares temporal decomposition (Appendix) which gives us three time traces that describe the best fitting amplitudes of these spectra to the data at each time. This procedure is iterated for each data set while the first two spectra are allowed to vary, such that they best fit (least-squares) the linear and transient spectra.

The resulting Gaussian spectra for the $4M$ $NaClO_4$ data set are shown as lines in Fig. 4. The $\nu=0\rightarrow1$ parts of these spectra are shown as dashed lines in the linear spectra of Fig. 1. Finally, the lines in Fig. 3 (top) show how these spectra, multiplied by their respective time traces, fit with the transient data for different times. The bottom of Fig. 3 shows the results of this same procedure for the $4M$ $HClO_4$ data set.

In our fitting procedure we find that the absorption bands of the bulk and anion bound populations are only slightly influenced by the exchange of sodium ions with protons. In principle, this exchange leads to a change of the electric field fluctuations, which could influence the absorption line shape of the O–D stretch vibrations. However these fluctuations are only strong for O–D groups that are directly connected to the proton as in HD_2O^+ and H_2DO^+. For those O–D groups the effect of the proton on the absorption line shape could be significant. However, for these O–D groups the vibrational lifetime is also very short, so that these O–D oscillators do not contribute to the signals at delay times >200 fs. The O–D oscillators that form the relatively narrow absorption bands near 2500 cm^{-1}, and that we observe in the time-resolved experiments, are at least one water molecule separated from the proton. For these $O-D\cdots O$ and $O-D\cdots ClO_4^-$ oscillators the effects of the protons on the line shape are negligible, as illustrated in Fig. 1.

B. Energy relaxation

The time traces that come out of the least-squares temporal decomposition are proportional to the populations $N_b(t)$ and $N_a(t)$. These are subsequently normalized at $t=0$ and shown in Fig. 5 for five different proton concentrations. We observe a clear dependence of the relaxation rate on acid concentration: with increasing acid concentration the relaxation becomes faster and nonexponential. The presence of the hydrated protons thus appears to open up an additional relaxation channel. While it may seem as if the added protons have more effect on the anion-bound water than the bulk, this is only because the anion bound water was slower to begin with and is more affected by an additional relaxation

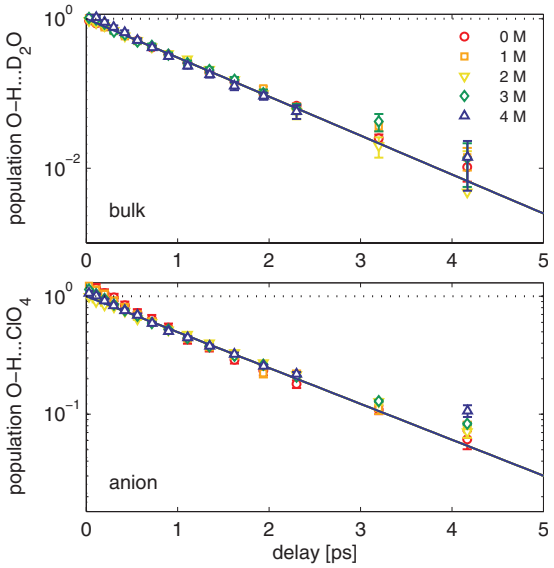

FIG. 6. Same as Fig. 5, but now for the bulk and anion bound O–H vibrations of HDO in D_2O at five different acid concentrations. The lines show the result of a global fit finding a bulk rate $k_b=1.2$ ps^{-1} and anion-bound rate $k_a=0.7$ ps^{-1}. The Förster transfer was found to be negligible (=0), using the same minimal transfer radius $a_0=1.5$ Å as for HDO in H_2O.

pathway. Finally, it may be noticed, especially for the anion bound water, that the decay rate for higher proton concentrations is still faster at delay times up to 5 ps. This means that the effect of the protons is still present at that time; otherwise the population traces would start to go parallel on this logarithmic scale.

To investigate the proton relaxation channel further, we perform an additional set of experiments in which we reverse the roles of hydrogen and deuterium. This time we use five aqueous solutions of HDO in D_2O at different ratios of (deuterated) perchloric acid ($DClO_4$) and sodium perchlorate ($NaClO_4$) and do the same pump-probe experiments as before, but now on the O–H stretching modes at 3400 cm^{-1}. This reciprocal system has one major difference: the O–H stretching frequency does not overlap spectrally with the deuteron (acid) background band, which lies at frequencies below the O–D stretching mode (2500 cm^{-1}). We find a decay time of 0.8 ps for the bulk O–H stretch, similar to a previously found value of 0.7 ps for neat HDO in D_2O.[6] The anion bound O–H stretch is again a bit slower with a vibrational relaxation time of 1.4 ps. Using the same procedure as before we show the time dependent population dynamics as a function of acid concentration in Fig. 6. Here we see a trend that is quite different from that of the O–D relaxation: the deuterons have no effect on the vibrational relaxation of the O–H stretch vibrations!

This clearly shows that the additional relaxation pathway observed for the O–D stretching mode, upon the addition of acid, is not the result of any changes in the hydrogen bond structure of the water but instead depends on spectral overlap (i.e., resonance) with modes associated with the dissolved proton. Schematically the flow of energy for the O–D may be drawn as in Fig. 7. We add another relaxation pathway from the O–D to the hydronium mode that is dependent on acid concentration and causes a speedup of the O–D relaxation

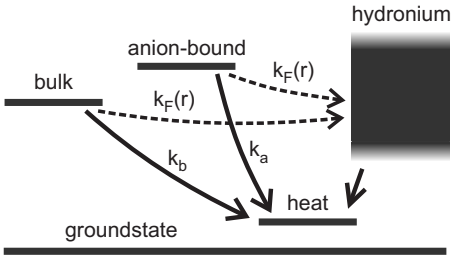

FIG. 7. Schematic energy level diagram. Arrows indicate channels for vibrational energy transfer. The relaxation rates of bulk (k_b) and anion-bound (k_a) water are mentioned in the text. The dashed arrows indicate the additional equilibration channels of Förster transfer to the hydronium band with distance dependent rate k_F.

rate. This proton associated mode decays very fast and is only observed indirectly through the thermalization spectrum and faster relaxation of the O–D.

There are several ways in which the vibrational energy may be transferred. One might think that the fast relaxation is associated with O–D vibrations in DH_2O^+ complexes. However, these directly contacting protons cause a significant redshift of the O–D stretch. By pumping and probing only at bulk O–D stretching frequencies, we automatically exclude these redshifted O–D stretch modes. For modes of H_3O^+ that are further away, vibrational energy can be transferred through resonant dipole-dipole coupling, i.e., Förster energy transfer (see Fig. 8).

We can exclude mechanisms different from Förster transfer from the comparison of the dynamics of the O–D oscillators in a H^+ rich environment with the dynamics of O–H oscillators in a D^+ rich environment. If the increase in relaxation rate would be due to a change in the fluctuating forces and/or nature of the accepting modes, the relaxation rate of the O–H oscillators would have been affected by the addition of D^+. This effect can be different from the effect of H^+ on the O–D oscillators, but some effect would have been expected. However, there is absolutely no effect of the addition of D^+ on the relaxation rate of the O–H oscillators. The Förster mechanism is the only mechanism that can explain this complete absence of an effect of D^+ on the O–H oscillators. In Fig. 5 the introduction of protons is observed to lead to an additional relaxation channel for the O–D vibra-

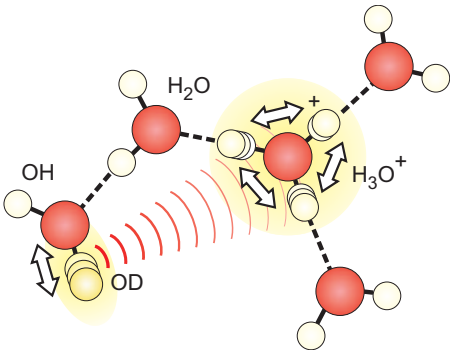

FIG. 8. Schematic representation of the Förster energy transfer process between the O–D stretch vibration and a nearby proton (associated) mode. White arrows indicate the direction of the transition dipole moments and the wavy lines represent the dipole field.

tion with a nonexponential time dependence. We will show in the following that this nonexponential effect can be very well explained by the Förster mechanism.

C. Förster transfer

In general, the rate of Förster transfer between two (oscillating dipole) modes a and b is proportional to the following expression:[19,32]

$$k_{F,a\to b} \sim \frac{\mu_a^2 \mu_b^2 \kappa_{ab}^2}{R_{ab}^6} \int \sigma_a(\nu)\sigma_b(\nu)d\nu. \tag{3}$$

In this expression μ_a and μ_b are the transition dipole moments of the transmitting and receiving dipole modes, $\kappa_{ab}=\cos\theta_{ab}-3\cos\theta_a\cos\theta_b$ is a geometrical factor expressing the relative orientations of the dipole moments, R_{ab} is the distance between the dipoles and σ_a and σ_b are the normalized vibrational line shapes of the two modes.

In modeling the data we describe the survival probability of O–D stretch modes which can relax their energy through a Förster transfer process to a radially uniform distribution of receiving proton (associated) modes. Once a transfer reaction has taken place, the energy is quickly dissipated by the proton mode[23] and this reaction is considered to be unidirectional. Since the Förster rate is highly dependent on distance, O–D modes that have protons in close proximity will show a higher energy transfer rate than those with protons at longer distances. Once the close configurations have reacted, the observed transfer rate, which is the sum of all configurations, will gradually slow down to that of the longer distance Förster transfer. This distance dependence will thus lead to a time dependent transfer rate and survival probability.

We will use the pseudounimolecular approximation to describe the time dependence of the survival probability. This approximation is valid since the concentration of accepting proton modes is much higher that of the excited O–D oscillators. An analogous treatment was previously used to describe diffusion controlled reaction rates,[33,34] electron transfer reactions[35] and acid base reactions in water.[36] The main difference is the functional form of the distance dependent reaction rate.

For simplicity, we assume that all parameters in Eq. (3), except R_{ab}, are independent of distance, and write the Förster rate as

$$k_F(r) = \frac{\hat{k}_F}{r^6}, \tag{4}$$

where $\hat{k}_F$ is the Förster rate for a single reaction pair at distance $r=1$, averaged over all orientations. Here we have assumed that the orientational factor κ_{ab} in Eq. (3) is uniform enough to be averaged out.

A population of Förster transmitters (O–D stretch) is placed in the origin ($r=0$) and we assume a radial distribution of receivers (proton modes) with initial concentration ρ for distances $>a_0$ (minimal transfer radius, i.e., excluded volume of the transmitter). The time and distance dependent concentration of unreacted pairs is described by

$$\frac{dC(r,t)}{dt} = -k_F(r)C(r,t),$$

$$C(r,0) = \rho, \quad r > a_0. \tag{5}$$

The solution to which equals

$$C(r,t) = \rho \exp\left(-\frac{\hat{k}_F}{r^6}t\right), \quad r > a_0. \tag{6}$$

The transfer rate between transmitters and receivers is dependent both on their separation distance [as in Eq. (4)] and proportional to the total amount of unreacted pairs at that distance

$$k_F(r,t) = k_F(r)C(r,t)4\pi r^2 dr. \tag{7}$$

To calculate the time dependent Förster rate $k_F(t)$ we integrate Eq. (7) over all distances $>a_0$

$$k_F(t) = \int_{r=a_0}^{\infty} k_F(r,t). \tag{8}$$

To obtain the Förster dependent survival probability $S_F(t)$ we integrate the time-dependent rate $k_F(t)$ over all times up to t

$$S_F(t) = \exp\left(-\int_0^t dt' k_F(t')\right). \tag{9}$$

Combining Eqs. (4)–(9) finally yields the survival probability of the O–D under the influence of Förster transfer to proton modes (concentration ρ)

$$S_F(t,\rho) = \exp\left(-\rho\int_{a_0}^{\infty} dr 4\pi r^2\left[1-\exp\left(-\frac{\hat{k}_F}{r^6}t\right)\right]\right). \tag{10}$$

In the absence of Förster transfer (no acid, $\rho=0M$), we have found that the O–D stretch for bulk and anion-bound water have standard decay rates $k_b=1/(1.7\ \text{ps})$ and $k_a=1/(4.3\ \text{ps})$, respectively. In terms of their respective survival probabilities S_b and S_a, we can write

$$S_b(t) = \exp(-k_b t), \tag{11}$$

$$S_a(t) = \exp(-k_a t). \tag{12}$$

Assuming that the standard and Förster relaxation processes constitute two parallel channels as shown in Fig. 7, the total population dynamics are proportional to the product of these two survival probabilities Eq. (10) and Eqs. (11) and (12)

$$S_{b,F}(t,\rho) = \exp\left(-k_b t - \rho\int_{a_0}^{\infty} dr 4\pi r^2\left[1-\exp\left(-\frac{\hat{k}_F}{r^6}t\right)\right]\right), \tag{13}$$

$$S_{a,F}(t,\rho) = \exp\left(-k_a t - \rho\int_{a_0}^{\infty} dr 4\pi r^2\left[1-\exp\left(-\frac{\hat{k}_F}{r^6}t\right)\right]\right). \tag{14}$$

These two equations have the following parameters: the bulk and anion decay rates k_b and k_a, that have already been ob-

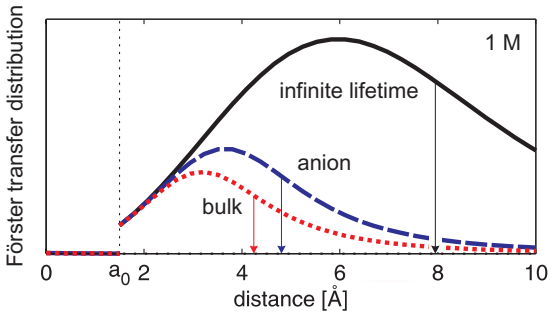

FIG. 9. Distance distribution of the Förster energy transfer events to hydrated protons for a proton concentration of $1M$ [Eq. (15)]. The solid line represents the distribution in case there would be no vibrational relaxation. The dashed and dotted curves represent the cases for which the donating O–D group is bonded to ClO_4^- ($T_1=4.3\pm0.3$ ps) and to H_2O ($T_1=1.7\pm0.1$ ps), respectively. The downward arrows indicate the average distances (first moments).

tained from the $0M$ proton data set. The concentrations ρ $(0-4M)$ are also known for each sample, which only leaves the Förster rate $\hat{k}_F$ and minimum radius a_0 to be determined. For this determination we use a global fit on all ten population decays (bulk and anion-bound for five concentrations). The results are shown as solid lines through the data points in Fig. 5. We have assumed, for simplicity that the Förster rate from the bulk and anion-bound populations is the same, an assumption that is justified given the broad and featureless profile of the proton background band. We find for the Förster rate between the O–D stretch and the proton associated modes $\hat{k}_F=1450$ ps^{-1} Å^6 and a minimum transfer radius a_0 of 1.5 Å. For the O–H stretch vibration, all concentrations fit well with a Förster rate of zero, as shown in Fig. 6 (taking the same value for a_0).

To get a molecular picture for the obtained rate of Förster transfer we calculate the distribution of Förster transfer events as a function of the distance between the donor O–D vibration and the acceptor hydrated proton vibrations $(1M)$. To obtain this distribution $D(r)$ we integrate the radial reactive flux $k_F(r,t)$ [Eq. (8)] weighted with the survival probability $S(t)$ over all times

$$D(r,\rho)dr = \int_0^\infty dt k_F(r,t)S(t,\rho)$$

$$= \frac{4\pi\hat{k}_F}{r^4}dr\int_0^\infty dt\,\exp\left(-\frac{\hat{k}_F}{r^6}t\right)S(t,\rho). \qquad (15)$$

The distance distribution of Förster transfer events $D(r,\rho)$, depends on the survival probability $S(t,\rho)$ through all channels, including the regular vibrational relaxation ($\rho=0$). We evaluate this function by numerical integration for three different scenarios. To evaluate the distribution for very slow vibrational relaxation ("infinite lifetime"), we use $S(t)$ from Eq. (10). For the bulk or anion-bound lifetimes, we use $S(t)$ given by Eq. (13) or Eq. (14), respectively. The three resulting distance distributions of Förster events are shown in Fig. 9. For the limiting case where there is no vibrational relaxation (infinite lifetime), the average distance over which energy transfer takes place equals about 8 Å. In the presence of the parallel vibrational relaxation process this distribution shifts to shorter distances, because for the longer distances the excitation has relaxed before energy transfer can occur. For the O–D bonded to H_2O and to ClO_4^-, we find average distances of 4.2 and 4.8 Å, respectively. These distances correspond to a separation between the donating O–D group and the hydrated proton of about two water molecules. This leads to the microscopic picture shown in Fig. 8. These distances are slightly larger than the corresponding Förster radii, $R_f=(\hat{k}_F/k_i)^{1/6}=3.7$ and 4.3 Å, because of the excluded volume ($a_0>1.5$ Å).

D. Implications

The present observations demonstrate that Förster energy transfer constitutes an effective long range coupling mechanism between vibrations, also of different character. Normally, interactions between different vibrations result from the anharmonic coupling of vibrational modes involving the same atoms of the molecule, meaning that this coupling is very local in character. In the present case, the interaction between different vibrational modes results from their long-range dipole-dipole coupling. This coupling leads to energy transfer between vibrational modes that are separated by several water molecules. For a proton at a distance of 4 Å we find a transfer rate of 0.35 ps^{-1}, which is comparable to the relaxation rate of the O–D vibration of HDO in pure water. This result shows that the dipole-dipole interactions to hydrated protons can be of similar strength as intramolecular anharmonic couplings. Hydrated protons are particularly efficient in this nonlocal interaction because of the large cross section of their vibrations. This large cross section is due to the large polarizability of the proton in water, i.e., the strong effect of (dipolar) electric fields on the positions and charges of the oxygen and hydrogen atoms of the hydrated proton solvation structures.

Hydrated protons will couple to all infrared-active molecular vibrations with frequencies between 1000 and 3400 cm^{-1}, because of the extremely large absorption bandwidth of the hydrated proton[20] (see also Fig. 1). The energy taken up by the proton vibrations will be quickly dissipated.[23] The combination of rapid dissipation and their role as highly efficient dipolar antennas makes protons into highly efficient nonlocal energy sinks in biochemical reactions. Biological systems are highly inhomogeneous and it is thus conceivable that a local proton would reside a few water molecules away from an affected molecular vibration. Finally, it should be noted that the coupling to hydrated protons does not rely on the excitation of the vibrational modes. The excitation of the vibrations only forms a very useful tool to measure the strength and distance dependence of this coupling. The dipole-dipole coupling is also present in the vibrational ground state and leads to a mixing of the character of the vibrational modes of the hydrated proton with the infrared-active modes of nearby molecular systems. This means that in aqueous media protons cannot only affect dissolved molecules by chemical interactions, i.e., (reversible) chemical binding, but also by mixing their vibrational character into the vibrational modes of the molecule.

IV. CONCLUSION

We investigated the energy relaxation pathways of O–D and O–H stretching modes in water with acid concentrations varying between 0 and $4M$ and perchlorate counter ions. Water molecules that form hydrogen bonds with the anion have a blueshifted spectrum compared to the bulk water. Using this spectral separation we measured the decay times for the bulk and anion-bound O–D stretch modes for the neutral sample to be 1.7 and 4.3 ps, respectively. Using the spectral signatures found in this data set we created a model independent set of population time traces for all acid concentrations. These time traces were seen to possess an additional time dependent decay rate for higher acid concentrations. This rate increase was fitted using a Förster transfer model, for all concentration, using a distance dependent rate of 1450 ps^{-1} $Å^6$ and a minimum transfer radius of 1.5 Å.

Using the same procedure on the reciprocal system of the O–H stretch in D_2O and varying concentrations of excess deuterons, no Förster transfer was observed. The bulk and perchlorate-bound decay times were found to be 0.8 and 1.4 ps, respectively, independent of acid concentration. This result shows that Förster transfer is not occurring for the O–H because it lacks spectral overlap with the dissolved deuteron background band.

We find evidence for energy transfer between vibrational modes that are separated by several water molecules. For a proton at a distance of about 4 Å the rate of Förster transfer is comparable to the relaxation rate of the O–D vibration of HDO in pure water.

ACKNOWLEDGMENTS

This work is part of the research program of the Foundation for Fundamental Research on Matter (FOM) which is financially supported by the Dutch organization for Scientific Research (NWO). The authors thank Hinco Schoenmaker for his technical support and Mischa Bonn for helpful comments on this manuscript.

APPENDIX: LEAST-SQUARES DECOMPOSITION

We assume that a data set $\Delta\alpha(t,\nu)$ can be described as the sum of constituent components. The response of each component i is the product of its population dynamics $N_i(t)$ and spectral signatures $\sigma_i(\nu)$

$$\Delta\alpha(t,\nu) = \sum_i N_i(t)\cdot\sigma_i(\nu). \tag{A1}$$

Decomposition will only be possible if either the population dynamics or spectral signatures are linearly independent from one component to the other.

We first calculate the spectral decomposition, i.e., a set of spectra $\sigma_i(\nu)$ that best fit a given set of population dynamics $N_i(t)$ to data points $\Delta\alpha(t,\nu)$ with standard deviations $\epsilon(t,\nu)$. To this end we define a function χ^2 that we need to minimize

$$\chi^2(\tilde{\sigma}_j) = \int dt\left(\frac{\Delta\alpha(t,\nu) - \Sigma_i N_i(t)\cdot\tilde{\sigma}_i}{\epsilon(t,\nu)}\right)^2, \tag{A2}$$

where $\tilde{\sigma}_i$ are now i separate variables that are proportional to the relative spectral amplitudes at frequency ν. The least-squares fitting linear combination can be calculated by equating the derivatives with respect to these amplitudes to zero

$$\frac{d}{d\tilde{\sigma}_i}\int dt\left(\frac{\Delta\alpha(t,\nu) - \Sigma_i N_i(t)\cdot\tilde{\sigma}_i}{\epsilon(t,\nu)}\right)^2 = 0. \tag{A3}$$

This gives us i equations with i unknowns that may be readily solved. Repeating this procedure for all frequencies results in i separate spectral signatures $\sigma_i(\nu)$.

Equivalently, this procedure will also work the other way around. If we know (or fit) the spectral signatures $\sigma_i(\nu)$, we can calculate the unknown population dynamics $\tilde{N}_i(t)$

$$\frac{d}{d\tilde{N}_i}\int d\nu\left(\frac{\Delta\alpha(t,\nu) - \Sigma_i \tilde{N}_i\cdot\sigma_i(\nu)}{\epsilon(t,\nu)}\right)^2 = 0. \tag{A4}$$

This will yield i time traces $N_i(t)$ that describe how a given set of spectra $\sigma_i(\nu)$ are individually evolving in data set $\Delta\alpha(t,\nu)$, without the need for any kinetic modeling or knowledge of initial conditions.

[1] L. D. Barron, L. Hecht, and G. Wilson, Biochemistry **36**, 13143 (1997).
[2] E. Meyer, Protein Sci. **1**, 1543 (1992).
[3] S. Woutersen and H. J. Bakker, Nature (London) **402**, 507 (1999).
[4] J. C. Deàk, S. T. Rhea, L. K. Iwaki, and D. D. Dlott, J. Phys. Chem. A **104**, 4866 (2000).
[5] M. L. Cowan, B. D. Bruner, N. Huse, J. R. Dwyer, B. Chugh, E. T. J. Nibbering, T. Elsaesser, and R. J. D. Miller, Nature (London) **434**, 199 (2005).
[6] Y. L. A. Rezus and H. J. Bakker, J. Chem. Phys. **125**, 144512 (2006).
[7] S. Woutersen, U. Emmerichs, H.-K. Nienhuys, and H. J. Bakker, Phys. Rev. Lett. **81**, 1106 (1998).
[8] J. Lindner, P. Vohringer, M. S. pshenichnikov, D. Cringus, D. A. Wiersma, and M. Mostovoy, Chem. Phys. Lett. **421**, 329 (2006).
[9] C. P. Lawrence and J. L. Skinner, J. Chem. Phys. **118**, 264 (2003).
[10] B. Auer, R. Kumar, J. R. Schmidt, and J. L. Skinner, Proc. Natl. Acad. Sci. U.S.A. **104**, 14215 (2007).
[11] T. Förster, Ann. Phys. **437**, 55 (1948).
[12] H. Graener, G. Seifert, and A. Laubereau, Chem. Phys. **175**, 193 (1993).
[13] H.-K. Nienhuys, R. A. Van Santen, and H. J. Bakker, J. Chem. Phys. **112**, 8487 (2000).
[14] J. Stenger, D. Madsen, P. Hamm, E. T. J. Nibbering, and T. Elsaesser, Phys. Rev. Lett. **87**, 027401 (2001).
[15] G. Gallot, S. Bratos, S. Pommeret, N. Lascoux, J. C. Leicknam, M. Kozinski, W. Amir, and G. M. Gale, J. Chem. Phys. **117**, 11301 (2002).
[16] J. B. Asbury, T. Steinel, K. Kwak, S. A. Corcelli, C. P. Lawrence, J. L. Skinner, and M. D. Fayer, J. Chem. Phys. **121**, 12431 (2004).
[17] J. D. Eaves, J. J. Loparo, C. J. Fecko, S. T. Roberts, A. Tokmakoff, and P. L. Geissler, Proc. Natl. Acad. Sci. U.S.A. **102**, 13019 (2005).
[18] C. Fang, A. Senes, L. Cristian, W. F. DeGrado, and R. M. Hochstrasser, Proc. Natl. Acad. Sci. U.S.A. **103**, 16740 (2006).
[19] M. Morin, P. Jakob, N. J. Levinos, Y. J. Chabal, and A. L. Harris, J. Chem. Phys. **96**, 6203 (1992).
[20] J. Kim, U. W. Schmitt, J. A. Gruetzmacher, G. A. Voth, and N. E. Scherer, J. Chem. Phys. **116**, 737 (2002).
[21] M. Eigen and L. D. Maeyer, Proc. R. Soc. London, Ser. A **247**, 505 (1958).
[22] D. Hadzi and S. Bratos, *The Hydrogen Bond* (Elsevier, New York, 1976), Vol. 2.
[23] S. Woutersen and H. J. Bakker, Phys. Rev. Lett. **96**, 138305 (2006).
[24] H. J. Bakker, Y. L. A. Rezus, and R. L. A. Timmer, J. Phys. Chem. A **112**, 11523 (2008).
[25] K. Tielrooij, C. Petersen, Y. Rezus, and H. Bakker, Chem. Phys. Lett. **471**, 71 (2009).

[26] G. Brink and M. Falk, Can. J. Chem. **48**, 3019 (1970).
[27] *Water: A Comprehensive Treatise*, edited by F. Franks (Plenum, New York, 1973), Vol. 3.
[28] A. W. Omta, A. M. Kropman, S. Woutersen, and H. J. Bakker, Science **301**, 347 (2003).
[29] J. B. Asbury, T. Steinel, C. Stromberg, S. A. Corcelli, C. P. Lawrence, J. L. Skinner, and M. D. Fayer, J. Phys. Chem. A **108**, 1107 (2004).
[30] J. C. Nash, *Compact Numerical Methods for Computers: Linear Algebra and Function Minimisation*, 2nd ed. (Taylor & Francis, Bristol, England, 1990).
[31] S. Park, M. Odelius, and K. J. Gaffney, J. Phys. Chem. B **113**, 7825 (2009).
[32] S. Woutersen, U. Emmerichs, and H. J. Bakker, J. Chem. Phys. **107**, 1483 (1997).
[33] M. Tachiya, Radiat. Phys. Chem. **21**, 167 (1983).
[34] A. Szabo, R. Zwanzig, and N. Agmon, Phys. Rev. Lett. **61**, 2496 (1988).
[35] Y. Lin, R. Dorfman, and M. D. Fayer, J. Chem. Phys. **90**, 159 (1989).
[36] M. J. Cox, R. L. A. Timmer, H. J. Bakker, S. Park, and N. Agmon, J. Phys. Chem. A **113**, 6599 (2009).